

1 A Hamiltonian Particle-Mesh Method for the Rotating Shallow Water Equations

Jason Frank¹, Georg Gottwald², and Sebastian Reich³

¹ CWI, P.O. Box 94079, 1090 GB Amsterdam, e-mail: jason@cwi.nl. [†]

² Department of Mathematics, University of Surrey, Guildford GU2 7XH, email: g.gottwald@surrey.ac.uk. [‡]

³ Department of Mathematics, Imperial College, 180 Queen's Gate, London, SW7 2BZ, email: s.reich@ic.ac.uk. [§]

Abstract. A new particle-mesh method is proposed for the rotating shallow-water equations. The spatially truncated equations are Hamiltonian and satisfy a Kelvin circulation theorem. The generation of non-smooth components in the layer-depth is avoided by applying a smoothing operator similar to what has recently been discussed in the context of α -Euler models.

1.1 Introduction

The interplay, in atmospheric flows, between high speed, divergence-dominated gravity waves and slowly advected vortical structures presents a challenge to numerical modelling. The quantity of principle interest, potential vorticity, is advected materially along particle paths, making particle methods an attractive option. However, to prevent the generation of spurious gravity waves, one must ensure that differentiated flow field variables remain smooth. Particle methods have the additional advantage of being Hamiltonian, with the well-known consequences for long time dynamics that follow from this. The application of artificial smoothing operators can destroy this property, though, if not done carefully.

A 2D model of the atmosphere which still retains the important dynamic interactions mentioned above is the rotating shallow-water equations (SWEs):

$$\frac{d}{dt}\mathbf{u} = -f_0\mathbf{u}^\perp - c_0\nabla_{\mathbf{x}}\eta, \quad (1.1)$$

$$\frac{d}{dt}\eta = -(1 + \eta)\nabla_{\mathbf{x}} \cdot \mathbf{u}, \quad (1.2)$$

[†] Partially supported by GMD, Bonn.

[‡] Supported by European Commission funding for the Research Training Network “Mechanics and Symmetry in Europe”.

[§] Partially supported by EPSRC Grant GR/R09565/01 and by European Commission funding for the Research Training Network “Mechanics and Symmetry in Europe”.

where $\mathbf{u} = (u, v)^T$ is the horizontal velocity field, $\mathbf{u}^\perp = (-v, u)^T$, $h = 1 + \eta$ is the normalized layer-depth variation, H_0 is the mean layer-depth (i.e. the total layer-depth is $H = H_0(1 + \eta)$), $f_0/2 > 0$ is the angular velocity of the reference plane, $c_0 := gH_0$ where $g > 0$ is the gravitational constant, and $\frac{d}{dt} = \frac{\partial}{\partial t} + \mathbf{u} \cdot \nabla_{\mathbf{x}}$ is the material time derivative [16].

The dynamical quantity of central importance in geophysical fluid dynamics is the potential vorticity (PV)

$$q = \frac{\zeta + f_0}{1 + h}, \quad \zeta = v_x - u_y = \nabla_{\mathbf{x}} \times \mathbf{u},$$

which is constant along particle trajectories; i.e. $dq/dt = 0$. Conservation of PV can be seen as a consequence of Kelvin's circulation theorem [16,6]:

$$\frac{d}{dt} \oint \left(\mathbf{u} + \frac{f_0}{2} \mathbf{x}^\perp \right) \cdot \mathbf{x}_s ds = 0,$$

where $\mathbf{x}(s)$ is a closed loop of materially advected particles, i.e.,

$$\frac{d}{dt} \mathbf{x}(s) = \mathbf{u}(\mathbf{x}(s)).$$

The importance attached to PV in atmospheric dynamics is evidenced by its central role in quasigeostrophic theory. In extra-tropical regions, the terms on the right hand side of (1.1) are nearly in balance. This motivates the definition of the geostrophic wind:

$$\mathbf{u}^g = \frac{c_0}{f_0} \nabla_{\mathbf{x}}^\perp \eta. \quad (1.3)$$

Note that if we assume (1.3), then the normalized layer-depth variation η can be recovered from the PV distribution via

$$(1 + \eta)q = \frac{c_0}{f_0} \nabla_{\mathbf{x}}^2 \eta + f_0. \quad (1.4)$$

Furthermore, the PV field itself is advected under the geostrophic flow field:

$$\frac{\partial q}{\partial t} + \mathbf{u}^g \cdot \nabla_{\mathbf{x}} q = 0. \quad (1.5)$$

The combined system (1.3), (1.4) and (1.5) is referred to as the quasigeostrophic approximation [16].¹ Note that the geostrophic wind \mathbf{u}^g is divergence-free and that it is assumed in general that solutions of the SWEs are nearly incompressible.

A large number of numerical methods for fluid flow simulations have been proposed over the years. We mention particle-in-cell (PIC) [8,3,9], smoothed-particle hydrodynamics (SPH) [14,15], finite mass [18,7], contour-advection

¹ Strictly speaking, the quasigeostrophic approximation makes use of a linearization of (1.4) to recover the geostrophic layer-depth from PV.

(CASL) [4], semi-Lagrangian and Eulerian methods [5]. None of these methods have been shown to simultaneously preserve energy (i.e. to be Hamiltonian), to advect PV (or to satisfy a circulation theorem), and to be numerically robust with respect to generation of unbalanced divergence $\delta = \nabla_{\mathbf{x}} \cdot \mathbf{u}$ [12] when applied to the SWEs (1.1)-(1.2). One of the most widely used methods for shallow water flows consists of a pseudospectral truncation of the Eulerian formulation in space combined with the leapfrog/trapezoidal rule (LF/TR) discretization in time [5,4]. Hyperdiffusion [4,5] is typically added to smooth the noise produced by the excitation of fine scale modes.

In this note we demonstrate that the standard SPH and PIC methods can be combined and appropriately modified so as to be Hamiltonian, advect PV properly, and to avoid instabilities associated with the finite precision of moving particle approximations.

1.2 The Hamiltonian Particle-Mesh (HPM) Method

We develop the proposed *Hamiltonian particle-mesh* (HPM) method in three steps. Ideas and concepts from PIC and SPH methods serve as a starting point. A crucial novel idea is the introduction of a smoothing operator which can either be interpreted as defining a globally supported basis function or as regularizing the layer-depth in the sense of α -Euler models [10].

1.2.1 Approximating the Continuity Equation

We start with the basic idea of smoothed particle hydrodynamics (SPH) [14] and approximate the total normalized layer depth $h = 1 + \eta$ by

$$h(\mathbf{x}, t) = \sum_k m_k \psi(\mathbf{x} - \mathbf{X}_k(t)), \quad (1.6)$$

where $\mathbf{X}_k(t)$, $k = 1, \dots, N$, are Lagrangian particle positions, $m_k > 0$ are constant weight factors, and $\psi(\mathbf{y}) \geq 0$ is an appropriate basis function [14,7]. Note that $h(\mathbf{x}, t)$ satisfies the continuity equation

$$h_t = -\nabla_{\mathbf{x}} \cdot (h\mathbf{v}),$$

with the velocity field \mathbf{v} defined via the partition of unity interpolation

$$\mathbf{v}(\mathbf{x}, t) = \frac{1}{h(\mathbf{x}, t)} \sum_k m_k \psi(\mathbf{x} - \mathbf{X}_k(t)) \frac{d}{dt} \mathbf{X}_k(t).$$

This provides us with an approximation to the continuity equation (1.2). See, for example, [18] for more details.

We now restrict the approximation $h(\mathbf{x}, t)$ to a regular grid with grid points $\mathbf{x}_{ij} = (i \cdot \Delta x, j \cdot \Delta y)$ and obtain

$$h^{ij} = \sum_k m_k \psi(\mathbf{x}_{ij} - \mathbf{X}_k(t)).$$

At this point we impose on the basis function ψ the requirement that

$$\sum_{i,j} \psi(\mathbf{x}_{ij} - \mathbf{x}) = 1 \quad (1.7)$$

for all \mathbf{x} and define

$$\psi_{ij}(\mathbf{x}) = \psi(\mathbf{x}_{ij} - \mathbf{x}).$$

The condition (1.7) guarantees conservation of the l_1 -norm of the layer-depth over the grid, i.e.

$$\sum_{i,j} h^{ij} = \sum_{i,j} \sum_k m_k \psi(\mathbf{x}_{ij} - \mathbf{X}_k(t)) = \sum_k m_k = \text{const.}$$

We mention that (1.7) is often used in PIC simulations to enhance the stability of the method [3]. More importantly, since the basis functions $\psi_{ij}(\mathbf{x})$ form a partition of unity, they can be used to interpolate the gridded layer-depth values back to all of $\mathbf{x} \in \mathbb{R}^2$, i.e.

$$h(\mathbf{x}, t) = h^{ij} \psi_{ij}(\mathbf{X}_k(t)), \quad (1.8)$$

where we have used the standard summation convention. We wish to emphasize that, due to approximation errors, the two formulas (1.6) and (1.8) lead to different results. While (1.6) is used in SPH-type methods, we will employ (1.8), which is closer to PIC approximation schemes.

1.2.2 Approximating the Momentum Equation

Let us assign to each Lagrangian particle a particle velocity

$$\mathbf{U}_k = \frac{d}{dt} \mathbf{X}_k, \quad (1.9)$$

$k = 1, \dots, N$. The momentum equation (1.1) is now discretized by

$$\frac{d}{dt} \mathbf{U}_k = -f_0 \mathbf{U}_k^\perp - c_0 \nabla_{\mathbf{x}} h(\mathbf{x}, t)|_{\mathbf{x}=\mathbf{X}_k}, \quad (1.10)$$

with h given by (1.8). The equations (1.9)-(1.10) form a closed set of equations.

We wish to mention, at this point, the important property

$$c_0 \nabla_{\mathbf{x}} h(\mathbf{x}, t)|_{\mathbf{x}=\mathbf{X}_k} = c_0 \sum_{i,j} h^{ij} \nabla_{\mathbf{X}_k} \psi_{ij}(\mathbf{X}_k) = \frac{1}{m_k} \nabla_{\mathbf{X}_k} \mathcal{V}(\{\mathbf{X}_l\}), \quad (1.11)$$

where

$$\mathcal{V}(\{\mathbf{X}_l\}) := \frac{c_0}{2} \sum_{i,j} h_{ij}^2 = \frac{c_0}{2} \sum_{i,j} \left(\sum_k m_k \psi_{ij}(\mathbf{X}_k) \right) \left(\sum_k m_k \psi_{ij}(\mathbf{X}_k) \right).$$

To be able to compute the divergence and vorticity of the velocity field we introduce gridded velocities via the partition of unity approximation:

$$\mathbf{u}^{ij} = \frac{\sum_k \mathbf{U}_k \psi(\mathbf{x}_{ij} - \mathbf{X}_k)}{\sum_k \psi(\mathbf{x}_{ij} - \mathbf{X}_k)}. \quad (1.12)$$

1.2.3 Global Basis Functions and Smoothing

From a computational complexity point of view, one would like to work with compactly supported basis functions such as product spline functions [2, 7]. But these basis functions seem to have the disadvantage of reduced accuracy and possible numerical instabilities over long time simulations. However, given a compactly supported basis function ψ , one can transform it into a globally supported basis function $\hat{\psi}$ via

$$\hat{\psi}(\mathbf{y}) := (1 - \alpha^2 \nabla_{\mathbf{y}}^2)^{-p} \psi(\mathbf{y}),$$

i.e., application of an inverse Helmholtz operator with smoothing length $\alpha > 0$ and an exponent $p > 0$. An efficient way to implement such an approach is to work on the given grid $\{\mathbf{x}_{ij}\}$ and to discretize the operator $\mathcal{H} = (1 - \alpha^2 \nabla_{\mathbf{x}}^2)^{-p}$ using spectral methods.² Let us denote the matrix representation of \mathcal{H} by H_{ij}^{nm} ; then we define

$$\hat{\psi}_{ij}(\mathbf{x}) := H_{ij}^{nm} \psi_{nm}(\mathbf{x}).$$

where we again use the standard summation convention. This modified basis function still satisfies

$$\sum_{i,j} \hat{\psi}_{ij}(\mathbf{x}) = 1.$$

Hence we obtain the layer-depth approximation

$$h(\mathbf{x}, t) = h^{ij} \hat{\psi}_{ij}(\mathbf{x}) = h^{ij} H_{ij}^{nm} \psi_{nm}(\mathbf{x}) = \hat{h}^{nm} \psi_{nm}(\mathbf{x}).$$

Thus changing the basis functions amounts to smoothing the gridded layer-depth values h^{ij} via

$$\hat{h}^{nm} := h^{ij} H_{ij}^{nm}. \quad (1.13)$$

This suggests replacing the discrete momentum equation (1.10) by the approximation

$$\frac{d}{dt} \mathbf{U}_k = -f_0 \mathbf{U}_k^\perp - c_0 \sum_{i,j} \hat{h}^{ij} \nabla_{\mathbf{x}_k} \psi_{ij}(\mathbf{X}_k). \quad (1.14)$$

The convolution (1.13) can be computed very efficiently using FFTs where

$$h^{ij} = \sum_k m_k \psi_{ij}(\mathbf{X}_k)$$

² Exact inversion of the Helmholtz operator is actually not required. Since we only aim at smoothing the high-frequency components, a few Jacobi iterations with a finite difference operator should be sufficient.

as before.

In a similar manner, one can introduce smoothed velocities

$$\hat{\mathbf{u}}^{nm} := \mathbf{u}^{ij} H_{ij}^{nm}. \quad (1.15)$$

There is an interesting link to the recently proposed α -Euler models for compressible and incompressible fluid flows. See [10] for an overview. While α -Euler models utilize a smoothed advection velocity field, it has been shown in [10] that this is equivalent to smoothing the pressure field in the case of incompressible fluids. What has been suggested in this section can be interpreted as smoothing the pressure field for a compressible flow. A stabilized SPH method based on a smoothed velocity field has been proposed in [13]. However, the associated equations of motion are more complex than standard SPH.

1.3 Conservation Properties

We show that the truncated equations are Hamiltonian and satisfy a Kelvin circulation theorem in the sense of [6].

First introduce the momenta

$$\mathbf{P}_k = m_k \mathbf{U}_k$$

and rewrite the equations (1.9) and (1.14) in the form

$$\frac{d}{dt} \mathbf{P}_k = -f_0 \mathbf{P}_k^\perp - c_0 m_k \sum_{i,j} \hat{h}^{ij} \nabla_{\mathbf{X}_k} \psi_{ij}(\mathbf{X}_k), \quad (1.16)$$

$$\frac{d}{dt} \mathbf{X}_k = \frac{1}{m_k} \mathbf{P}_k, \quad (1.17)$$

$k = 1, \dots, N$. Using a slight modification of (1.11) it is easy to verify that these equations are canonical [1] with Hamiltonian

$$\mathcal{E} = \sum_k \frac{\mathbf{P}_k \cdot \mathbf{P}_k}{2m_k} + \frac{c_0}{2} \sum_{i,j} h^{ij} \hat{h}^{ij}, \quad (1.18)$$

where one uses the fact that H_{nm}^{ij} is symmetric. The structure matrix J consists of N copies of

$$J_k = \begin{bmatrix} -f_0 J_2 & -I_2 \\ I_2 & 0_2 \end{bmatrix}, \quad J_2 = \begin{bmatrix} 0 & -1 \\ 1 & 0 \end{bmatrix},$$

along its main diagonal.

We mention that the Hamiltonian (energy) \mathcal{E} is similar to the discrete energy obtained from a finite mass method [7] discretization with the spatial

integral performed using a simple Riemann sum and no rotational degrees of freedom included.

As shown previously, the method conserves the l_1 -norm of the layer-depth approximations $h^{ij}(t)$ and $\widehat{h}^{ij}(t)$, respectively.

Let us now assume that, at time $t = 0$, a continuous velocity field $\mathbf{U}(\mathbf{x})$ is given and that $\mathbf{U}_k(0) = \mathbf{U}(\mathbf{X}_k(0))$. Once the solutions to the finite-dimensional equations (1.16)-(1.17) have been computed, the velocity field $\mathbf{U}(\mathbf{x})$ can, in principle, be advected according to

$$\begin{aligned} \frac{d}{dt}\mathbf{U}(\mathbf{X}) &= -c_0 \nabla_{\mathbf{x}} h(\mathbf{x}, t)|_{\mathbf{x}=\mathbf{X}}, & h(\mathbf{x}, t) &= \sum_{ij} \widehat{h}^{ij}(t) \psi_{ij}(\mathbf{x}), \\ \frac{d}{dt}\mathbf{X} &= \mathbf{U}(\mathbf{X}). \end{aligned}$$

Note that

$$\mathbf{U}(\mathbf{X}_k(t)) = \mathbf{U}_k(t)$$

for all $t \geq 0$. Now let us also advect a loop of points $\mathbf{X}(s, t)$ along the velocity field $\mathbf{U}(\mathbf{X}(s, t))$, i.e.,

$$\frac{d}{dt}\mathbf{X}(s) = \mathbf{U}(\mathbf{X}(s)).$$

If a Lagrangian particle \mathbf{X}_k is part of the loop at $t = 0$, then it will remain on the loop for all $t \geq 0$. Furthermore, along the given loop, Kelvin's circulation theorem

$$\frac{d}{dt} \oint \left(\mathbf{U} + \frac{f_0}{2} \mathbf{X}^\perp \right) \cdot \mathbf{X}_s ds = 0 \quad (1.19)$$

holds as can be verified by straightforward differentiation. Note that (1.19) does not imply advection of PV in the standard sense. See [6] for more details.

1.4 Time-Stepping

We use a second-order symplectic method [17] in time based on a three-term splitting of the Hamiltonian \mathcal{E} into

$$\mathcal{E} = \frac{1}{2}\mathcal{T} + \mathcal{V} + \frac{1}{2}\mathcal{T},$$

where

$$\mathcal{T} = \sum_k \frac{\mathbf{P}_k \cdot \mathbf{P}_k}{2m_k}, \quad \mathcal{V} = \frac{c_0}{2} \sum_{i,j} h^{ij} \widehat{h}^{ij},$$

and composition of the associated flow maps [11].

1.5 Numerical Experiment

We applied the new method to the SWEs on $[0, 2\pi)^2$ with periodic boundary conditions. On the $n \times n$ grid, we defined tensor product basis functions

$$\psi(\mathbf{x}) = \phi\left(\frac{x}{\Delta x}\right) \cdot \phi\left(\frac{y}{\Delta y}\right), \quad \Delta x = \Delta y = \frac{2\pi}{n},$$

where $\phi(r)$ is the cubic spline

$$\phi(r) = \begin{cases} \frac{2}{3} - |r|^2 + \frac{1}{2}|r|^3, & |r| \leq 1 \\ \frac{1}{6}(2 - |r|)^3, & 1 < |r| \leq 2 \\ 0, & |r| > 2 \end{cases}.$$

Initially, the $N = (6 \cdot n)^2$ particles also were positioned on a uniform grid.

The programs were written in *MATLAB* except for the particle-grid interpolation operators which were implemented as *mex* codes in C.

The parameters in (1.1) were chosen to be $c_0 = 4\pi^2$ and $f_0 = 2\pi$, so that time $T = 1$ corresponds to one planar rotation (one “day”). This combination implies a Rossby deformation radius $L_R = \sqrt{c_0}/f_0 = 1$.

The initial layer depth was defined by

$$h(\mathbf{x}, 0) := \frac{1}{1 + \Delta q(\mathbf{x})} + \kappa,$$

where κ is chosen so that $\text{mean}(h) = 1$ and

$$\Delta q(\mathbf{x}) = \frac{1}{\pi}(y - \pi)e^{-2(y - \pi)^2} \left(1 + \frac{1}{10} \sin 2x\right).$$

This layer depth, coupled with the initially geostrophic velocity field

$$\mathbf{u}^\perp(\mathbf{x}, 0) := -\frac{c_0}{f_0} \nabla_{\mathbf{x}} h(\mathbf{x})$$

obtained via (1.11), simulates an unstable jet similar to that considered in [4].

Integration was performed until time $T = 15$, using a stepsize $\Delta t = 1/100$. We used $\alpha = 2L/n$ and $p = 1$ for the smoothing operator \mathcal{H} .

As a check on convergence we also computed the solution using a simple pseudospectral discretization on a 128×128 grid, including a small hyperdiffusion term. A contour plot of potential vorticity is shown in Fig. 1.1.

The time evolution of the PV field as computed by the HPM method is displayed in Fig. 1.2. To produce this figure, we computed the PV distribution on the grid at time $t = 0$ using

$$Q^{ij} = (D_x \hat{v} - D_y \hat{u})^{ij} / \hat{h}^{ij}, \quad (1.20)$$

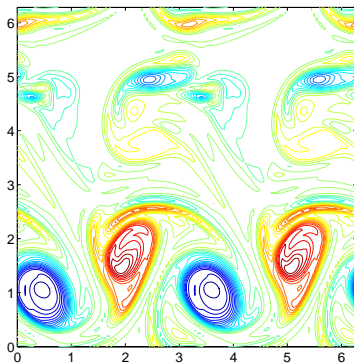


Fig. 1.1. Contours of potential vorticity at time $t = 15$ obtained with a pseudospectral discretization, $n = 128$.

where D_x and D_y represent the discrete spectral derivatives in the x and y directions, resp., and $\hat{\mathbf{u}} = (\hat{u}, \hat{v})$ is the smoothed velocity (1.15). Next we extended this PV field to the particles using an interpolation analogous to (1.8). The resulting particle PV values were then fixed for the duration of integration, and interpolated back to the grid using (1.12) when output was desired. It is interesting to compare the PV field obtained in this manner with that obtained by directly applying (1.20) at output intervals. The result for $t = 15$ can be found in Fig. 1.3. The agreement with the corresponding field in Fig. 1.2 is remarkable, and suggests that PV is very consistently advected along particle paths of HPM, despite any explicit enforcement of this.

Due to the absence of hyperdiffusion in this computation, small scale vortical structures appear, but the large scale structures evolve as in Fig. 1.1.

In Fig. 1.4 we have plotted the error in the Hamiltonian (1.18). In the figure, this error is scaled by the usable energy, defined as

$$\mathcal{E}_{\text{base}} = \mathcal{E}(t = 0) - \mathcal{E}(u \equiv 0, v \equiv 0, h \equiv 1).$$

In the figure the energy is well conserved, in keeping with known results for symplectic integrators. Since (1.18) is a first integral of the dynamics (1.16) and (1.17), this error can be made as small as desired by reducing the timestep Δt .

Also in Fig. 1.4 we have plotted the mean divergence level, defined as the l^2 -norm

$$\|\delta\| = \left(\sum_{i,j} (\delta^{ij})^2 \Delta x \Delta y \right)^{1/2},$$

where δ^{ij} is the divergence of the smoothed velocity field (1.15).

The mean divergence level is a measure of the degree of balance in the flow. It is important to observe that $\|\delta\|$ remains rather flat, indicating that gravity wave activity is not increasing in magnitude.

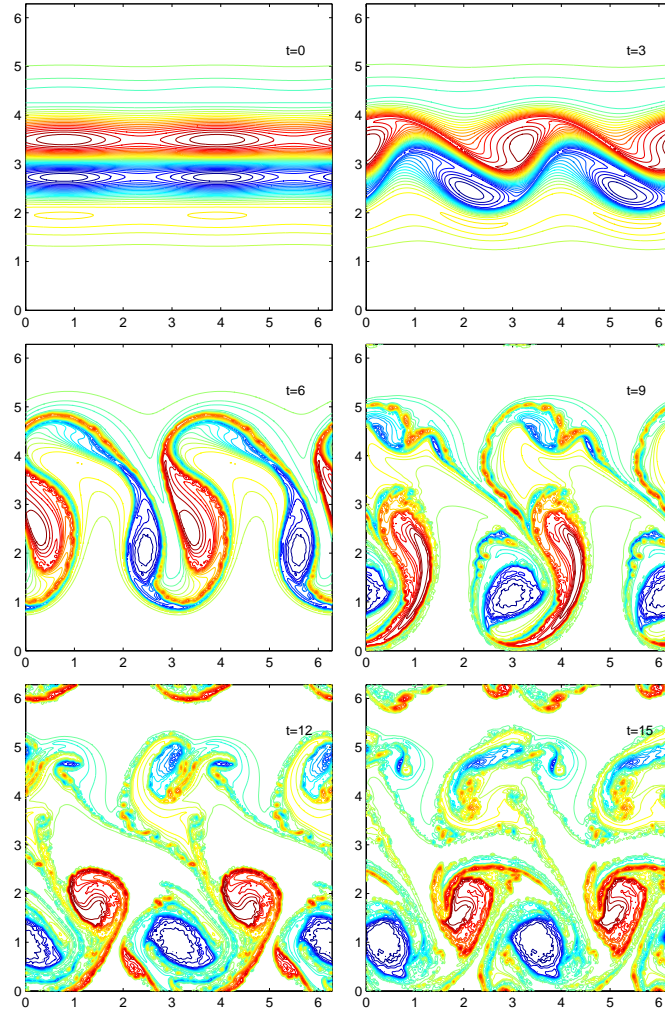


Fig. 1.2. Contours of potential vorticity on intervals of 3 days.

1.6 Conclusion

The Hamiltonian particle-mesh method seems to be applicable to more sophisticated geophysical fluid models such as the primitive equations and the SWEs on the sphere [16]. What is required next is a very careful comparison with contour-advection (CASL) algorithms and standard pseudospectral codes in terms of accuracy, applicability, and efficiency.

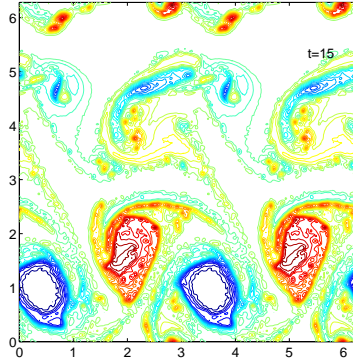


Fig. 1.3. Smoothed Eulerian potential vorticity at time $t = 15$

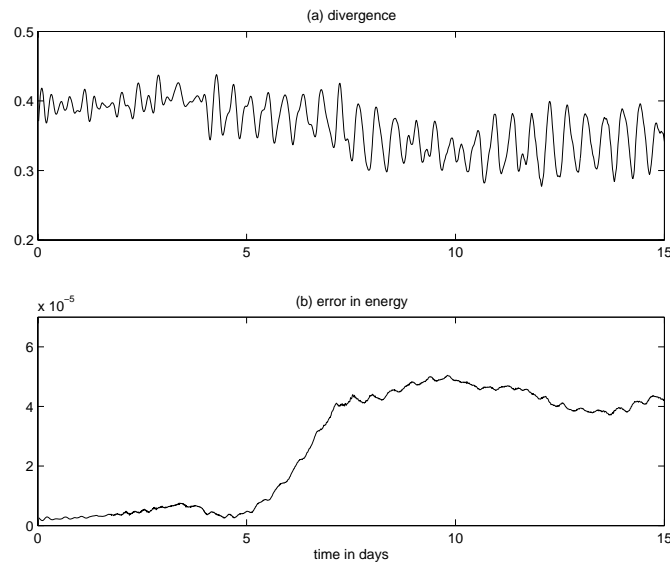


Fig. 1.4. Evolution of (a) the mean divergence level and (b) the Hamiltonian error over the simulation interval.

References

1. V. I. ARNOLD, *Mathematical Methods of Classical Mechanics*, Springer-Verlag, 1978.
2. C. DE BOOR, *A practical guide to splines*, Springer-Verlag, 1978.
3. J. BRACKBILL & H. RUPPEL, *Flip: a method for adaptively zoned particle in cell calculations of fluid flows in two dimensions*, J. Comput. Phys. **65**, 1986, 314–343.
4. D.G. DRITSHEL, L.M. POLVANI, & A.R. MOHEBALHOJEH, *The contour-advective semi-Lagrangian algorithm for the shallow water equations*, Mon. Weather Rev. **127**, 1999, 1551–1565.

5. D.R. DURRAN, *Numerical Methods for Wave Equations in Geophysical Fluid Dynamics*, Springer-Verlag, New York, 1999.
6. J.E. FRANK & S. REICH, *Conservation properties of smoothed particle hydrodynamics applied to the shallow water equations*, submitted.
7. CH. GAUGER, P. LEINEN, & H. YSERENTANT, *The finite mass method*, SIAM J. Numer. Anal. **37**, 1768–1799, 2000.
8. F.H. HARLOW, *The particle-in-cell computing methods for fluid dynamics*, Methods Comput. Phys. **3**, 1964, 319–343.
9. R. W. HOCKNEY & J. W. EASTWOOD, *Computer Simulation Using Particles*, Adam Hilger, Bristol, New York, 1988.
10. D. D. HOLM, *Fluctuation effects on 3D Lagrangian mean and Eulerian mean fluid motion*, Physica D **133**, 1999, 215–269.
11. R.I. MCLACHLAN, *On the numerical integration of ODEs by symmetric composition methods*, SIAM J. Sci. Comput. **16**, 1995, 151–168.
12. A. R. MOHEBALHOJEH & D. G. DRITSCHEL, *On the representation of gravity waves in numerical models of the shallow-water equations*, Q. J. R. Meteorol. Soc. **126**, 2000, 669–688.
13. J. J. MONAGHAN, *On the problem of penetration in particle methods*, J. Comput. Phys. **82**, 1989, 1–15.
14. J. J. MONAGHAN, *Smoothed particle hydrodynamics*, Ann. Rev. Astron. Astrophys. **30** (1992), 543–574.
15. R. SALMON, *Practical use of Hamilton's principle*, J. Fluid Mech. **132**, 431–444, 1983.
16. R. SALMON, *Lectures on Geophysical Fluid Dynamics*, Oxford University Press, Oxford, 1999.
17. J.M. SANZ-SERNA & M.P. CALVO, *Numerical Hamiltonian Problems*, Chapman & Hall, London, 1994.
18. H. YSERENTANT, *A new class of particle methods.*, Numer. Math. **76**, 1997, 87–109.